



Likelihood parameter estimation for calibrating a soil moisture model using radar backscatter

Grey S. Nearing^{a,*}, M. Susan Moran^b, Kelly R. Thorp^c, Chandra D. Holifield Collins^b, Donald C. Slack^a

^a University of Arizona, Department of Agricultural and Biosystems Engineering, Tucson AZ, United States

^b USDA-ARS Southwest Watershed Research Center, Tucson AZ, United States

^c USDA-ARS Arid Lands Agricultural Research Center, Maricopa AZ, United States

ARTICLE INFO

Article history:

Received 12 May 2009

Received in revised form 24 May 2010

Accepted 24 May 2010

Keywords:

Synthetic aperture radar

Parameter estimation

Soil moisture remote sensing

ABSTRACT

Land surface model parameter estimation can be performed using soil moisture information provided by synthetic aperture radar imagery. The presence of speckle necessitates aggregating backscatter measurements over large (>100 m × 100 m) land areas in order to derive reliable soil moisture information from imagery, and a model calibrated to such aggregated information can only provide estimates of soil moisture at spatial resolutions required for reliable speckle accounting. A method utilizing the likelihood formulation of a probabilistic speckle model as the calibration objective function is proposed which will allow for calibrating land surface models directly to radar backscatter intensity measurements in a way which simultaneously accounts for model parameter- and speckle-induced uncertainty. The method is demonstrated using the NOAH land surface model and Advanced Integral Equation Method (AIEM) backscatter model calibrated to SAR imagery of an area in the Southwestern United States, and validated against in situ soil moisture measurements. At spatial resolutions finer than 100 m × 100 m NOAH and AIEM calibrated using the proposed radar intensity likelihood parameter estimation algorithm predict surface level soil moisture to within 4% volumetric water content 95% of the time, which is an improvement over a 95% prediction confidence of 10% volumetric water content by the same models calibrated directly to soil moisture information derived from synthetic aperture radar imagery at the same scales. Results suggest that much of this improvement is due to increased ability to simultaneously estimate NOAH parameters and AIEM surface roughness parameters.

© 2010 Elsevier Inc. All rights reserved.

1. Introduction

A standardized target set of accuracy and precision requirements governing the reporting of soil moisture distribution for watershed-scale applications is outlined by Moran et al. (2004). Such information would optimally be available at a fine spatial resolution of between 10 and 100 m, with coverage areas at the watershed scale or larger. Because many management decisions are made on a day-to-day basis, product delivery requirements are stringent and delivery would optimally be available immediately upon request.

Difficulties arise in using field-based measurements of soil moisture to meet these requirements since soil water distributions are highly heterogeneous in nature (Mohanty et al., 2002) and field measurements offer only single-point information. Alternatively, satellite-based synthetic aperture radar (SAR) observation systems can be used to make soil moisture measurements continuously over

large areas; radar can penetrate the land surface to a depth dependent on wavelength, and SAR imagery can be obtained at spatial resolutions finer than soil moisture product requirements. The sensitivity of radar backscatter signal to soil moisture is due to the difference in permittivity, or dielectric constant, of dry and wet soils (Ulaby, 1974; Dobson et al., 1985), thus moisture information contained in the radar signal is limited by the depth of surface penetration and confined to the top few centimeters of soil (Nolan & Fatland, 2003). Additionally, the potential for SAR imagery to provide soil moisture information at the required spatial resolution is hampered by the presence of speckle, which is not affected by soil water content. Typically accounting for speckle is done statistically through a *multilook* process by spatially aggregating SAR image pixels over a homogeneous area (Oliver & Quegan, 1998 pp 28–29). In order to extract reliable soil moisture information from a SAR image, it is necessary to aggregate backscatter measurements over areas large enough to compromise the ability of the imagery to provide a soil moisture information product with the required spatial resolution (Thoma et al., 2008). Also, because of infrequent revisit coverage by high resolution satellite SAR systems (on the order of a few days to weeks), imagery fails to provide the continuous coverage needed to

* Corresponding author.

E-mail address: grey@email.arizona.edu (G.S. Nearing).

track short-term soil moisture behavior and cannot deliver up-to-date information between satellite overpasses.

While SAR imagery can provide instantaneous measurements of surface level soil moisture, hydrologic land surface models (LSMs) are able to provide continuous soil moisture time series with accuracies that are largely dependent on appropriate parameterization. It is reasonable to assume that a LSM parameterized so that predictions of soil moisture closely match the available SAR image estimations will also be able to reasonably predict soil moisture behavior between available imagery. The idea of parameterizing a LSM using system observations has been studied extensively in general (e.g. Johnston & Pilgrim, 1976; Sorooshian & Gupta, 1985; Yapo et al., 1998; Liu & Gupta, 2007) and with specific regard to soil moisture prediction (e.g. Burke et al., 1997; Feddes et al., 1993; Mertens et al., 2006; Santanello et al., 2007; Ines & Mohanty, 2008, 2009; Peters-Lidard et al., 2008; Pauwels et al., 2009). In addition, it has been suggested that it may be possible to use models calibrated to surface level soil moisture information to retrieve reliable sub-surface information (Calvet & Noilhan, 2000).

Calibrating a model to system observations involves the minimization of a measure of disagreement between the modeled time series and the observed state – in this case soil moisture content. An objective function will have the general form

$$\gamma = f(O, Z), \quad (1)$$

where γ is an aggregate measure of disagreement characterized by the relationship $f(\cdot)$ between modeled (output) values at all of T time steps, $O = \{o_1, o_2, \dots, o_T\}$, and system observations at corresponding time steps, $Z = \{z_1, z_2, \dots, z_T\}$. Recognizing that O is functionally dependent on the R model parameters, $\Theta = \{\theta_1, \theta_2, \dots, \theta_R\}$, and the model forcing data, $F = \{f_1, f_2, \dots, f_K\}$ at $K \geq T$ time steps, according to the model structural equations, $M(\cdot)$,

$$O = M(F, \Theta), \quad (2)$$

Eq. (1) can be characterized as

$$\gamma = f(M(F, \Theta), Z) = f_M(F, \Theta, Z) = f_{M,F,Z}(\Theta) \quad (3)$$

where $f_M(\cdot)$ is obtained by considering $M(\cdot)$ constant, and $f_{M,F,Z}(\cdot)$ further depends on the assumption that the forcing and observation data are known and independent of the model. Thus, disagreement (γ) is minimized by adjusting model parameter values. An objective function should characterize a relationship which is related to agreement between modeled predictions and system observations; the choice of the definition of agreement and the choice of objective function are often subjective and application dependent (Diskin & Simon, 1977). Often the mean-squared-error (MSE) between modeled and observed data is used and agreement is maximized when the objective function has a minimum value.

Once disagreement is minimized by adjusting model parameters, the set of estimated parameters can be used to produce continuous model output which, assuming accurate model structure, forcing data and observations, can be taken as a reliable representation of the system. The output of the calibrated LSM will be continuous at the temporal resolution of the forcing data and has the potential for modeling soil water behavior. However, behavior of the system at spatial scales smaller than the observations cannot be distinguished by this procedure and calibrated model output will be limited to the spatial resolution of the observations. Therefore, a distributed LSM calibrated using multilook-derived soil moisture measurements will have the potential to produce a soil moisture map that meets temporal and spatial coverage requirements but not the spatial resolution requirement. The objective of this work is to develop an alternative technique for merging SAR imagery with LSMs through parameter estimation which will increase the reliability of calibrated-

model soil moisture predictions at spatial resolutions fine enough to meet product requirements.

2. Models, study site, and methods

The alternative proposed here involves directly comparing SAR backscatter intensity to that provided by an LSM outputting a theoretical backscatter intensity time series dependent on system parameters and surface level soil moisture (similar to Burke et al., 1997). A LSM is constructed to report theoretical non-speckled radar backscatter intensity values and a likelihood relationship between these pure information values and speckle-affected real SAR intensity images is used as the objective function. The result of this calibration procedure is a maximally-likely modeled soil moisture time series considering parameter uncertainty and speckle uncertainty. In this manuscript the technique is presented and demonstrated 1) with sets of artificial, model-produced soil moisture data and simulated speckled SAR imagery to show that the theory is sound in the absence of model error and 2) with SAR imagery of a sparsely vegetated area in the Southwestern United States. The results of the real imagery demonstration are validated against in-situ soil moisture measurements. Performance is compared to that of a model calibrated to in-situ data in order to assess the effects of observation data noise on the procedure, and to models calibrated with soil moisture derived from individual SAR images using a multilook technique in order to assess any improvement offered by the likelihood approach.

2.1. The advanced integral equation backscatter model

Radar backscatter, as measured by SAR satellites, is mostly dependent on four land surface characteristics: topography, surface roughness, soil moisture and vegetation. In order to accurately model a backscatter intensity signal all of these factors must be accounted for along with instrument properties and viewing geometry. One of the most widely used theoretical representations of a radar backscatter signal from bare soils is the integral equation method (IEM; Fung et al., 1992) which accounts for all of the relevant parameters except topography. For this study the landscape is considered flat. The IEM requires two surface roughness parameters – root mean squared surface height (h_{rms} [cm]), which is defined for an N -point discrete surface profile with surface heights z_i as

$$h_{rms} = \sqrt{\left(\frac{1}{N}\right) \sum_{i=1}^N \left(z_i - \left(\frac{1}{N}\right) \sum_{j=1}^N z_j\right)^2}, \quad (4)$$

and correlation length (C_L [cm]), which describes the relative spatial dependence of roughness; in this case an exponential autocorrelation function is used. In addition, the IEM requires viewing angle, radar signal frequency (in part used to scale surface roughness parameters with respect to wavelength), and the soil dielectric constant. Assuming that the sand and clay fractions of the soil are known the dielectric constant, $\epsilon \in \mathbb{C}$, can be approximated as a function of soil moisture in terms of volumetric water content (VWC) using the Hallikainen et al. (1985) polynomial expressions (HPE):

$$\begin{aligned} \epsilon_{real} &= (1.993 + 0.002 * S + 0.015 * C) \\ &\quad + (38.086 - 0.176 * S - 0.633 * C) * \phi_v \\ &\quad + (10.72 + 1.256 * S + 1.522 * C) * \phi_v^2 \\ \epsilon_{im} &= (-0.123 + 0.002 * S + 0.003 * C) \\ &\quad + (7.502 - 0.058 * S - 0.116 * C) * \phi_v \\ &\quad + (2.942 + 0.452 * S + 0.543 * C) * \phi_v^2 \end{aligned} \quad (5)$$

Where ϕ_v is volumetric water content of the soil, S is the sand fraction (%) and C is the clay fraction (%).

The advanced version of the IEM (AIEM) is used here and improves on theoretical results of the IEM in general, and especially over rougher surfaces (Chen et al., 2003). Performance is highly sensitive to the surface roughness parameterization (Fig. 1) (Altese et al., 1996; Bryant et al., 2007); it is essential to use parameter values which well-represent the imaged area (Fung et al., 1996). Many efforts have been made to measure and parameterize surface roughness. Both ground-based (e.g. Podmore & Huggins, 1981; Baghdadi et al., 2000; Mattia et al., 2003; Oelze et al., 2003; Bryant et al., 2007; Oh & Hong, 2007) and satellite-based methods (e.g. Baghdadi et al., 2002a,b; Zribi & Dechambre, 2003; Rahman et al., 2008) have been proposed, however in general it is not possible to visit every location where soil moisture estimates are needed and satellite-based methods are necessary. A comprehensive discussion of problems related to modeled backscatter dependency on surface roughness parameterization is given by Verhoest et al. (2008).

In addition to what can be modeled using the AIEM, SAR backscatter is affected by constructive and destructive interference of signal from discrete scatterers within a given pixel which manifests in imagery as *speckle* and can be modeled in a probabilistic fashion (Goodman, 1975). If all of the non-speckle related parameters including VWC are known and backscatter is modeled, disregarding any model error, the difference between this modeled behavior and SAR imagery can be attributed to speckle. However, if a given set of parameters is not known and many samples (images of a static, homogeneous area) are available, then the probabilistic speckle model can be used to find maximum likelihood estimators of the unknown parameters. This is a very useful and often employed technique for despeckling SAR imagery (Oliver & Quegan, 1998 p. 162), and is a form of multilooking because it assumes homogeneity over a given area. Because soil moisture cannot generally be considered constant between satellite overpasses, the homogeneity requirement would preclude sampling from sequential images of a land surface area. Thus, the sample set used in this sort of parameter estimation procedure is necessarily comprised of pixels from a single overpass image representing an area which is assumed to be homogeneous in soil moisture content, surface roughness, topography and vegetation.

By estimating the AIEM parameters relevant to each of several SAR images of a given land surface area from different overpass times a maximally-likely soil moisture time series can be found as long as an adequate homogeneous area is imaged during each overpass. If there is no correlation between members of the soil moisture time series,

then the required number of samples from each overpass image — or equivalently, the size of the area to be considered homogeneous — is equal to that required in the single image case. If, however, there is correlation between soil moisture at different times in the series then this can be exploited to reduce the number of independent samples needed to derive a maximally-likely estimate of the soil moisture time series.

2.2. The NOAH land surface model

Correlation between soil moisture values at different times can be described by a soil moisture model which accounts for earth processes affecting water exchange in the soil. Soil moisture models take many forms with varying levels of complexity and have been designed for many purposes. The NOAH community land surface model, which at its core contains a soil moisture accounting scheme, is a reliable land surface hydrology model (Mahrt & Pan, 1984; Ek et al., 2003) functioning as a 1-dimensional soil column simulator. NOAH optimally accepts sub-hourly forcing data in the form of atmospheric conditions including precipitation, and returns an array of flux and state variable time series including volumetric water content.

The NOAH structure used in this study has six vegetation parameters, four soil texture parameters, one topographic slope parameter, a number of soil layers to be simulated along with the depths of each, and a monthly green vegetation fraction (GVF; Gutman & Ignatov, 1998) vector. Soil, and vegetation parameters (Table 1) are considered not known and estimated using an automatic calibration method. For this study, the number of soil layers is held constant at four with depths of (from top down) 0.05 m, 0.25 m, 0.6 m and 1.0 m for a combined depth of 1.9 m. Satellite-derived GVF data is made available by the NOAA STAR long term greenness fraction database (Jiang et al., 2009).

NOAH requires initial states in the form of average soil moisture and soil temperature for all modeled soil layers as well as temperature of the soil surface, snow depth and snow water equivalent, and canopy water content. Improper initialization of model states can significantly bias seasonal model output (Koster et al., 2004). Rodell et al. (2005) suggests a method, which is used here, for initializing land surface models. Forcing data spanning eight years (described below) and NOAH parameters considered default parameters (Table 1, column 3; Hogue et al., 2005) are available for implementing this initialization procedure to include a 446 day spin-up period and to subsequently

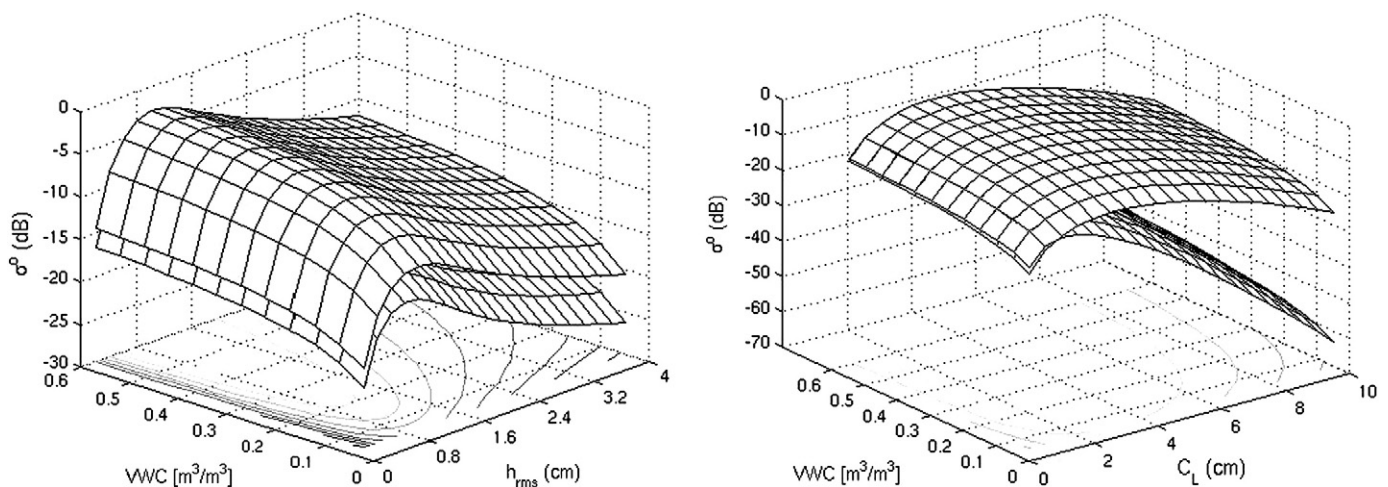


Fig. 1. AIEM (coupled with HPE) modeled HH backscatter (σ^0 ; decibels) response to varying (left) soil volumetric water content (VWC) and root-mean-squared surface roughness height (h_{rms}) where the two contour surfaces represent C_L values of 1.25 cm [top] and 0.76 cm [bottom]. Backscatter response (right) to VWC and surface roughness correlation length (C_L) where the two contour surfaces represent h_{rms} values used in artificial and real data calibrations $h_{rms} = 1.48$ cm, $h_{rms} = 0.57$ cm respectively. The behavior of VV response is similar, with a notable difference being a positive response shift with constant h_{rms} , C_L .

Table 1
NOAH parameterization, initialization parameter values and calibration intervals.

Parameter name	Description	NOAH initialization value	Lower bound	Upper bound
smcmax	Maximum soil moisture content (m ³ /m ³)	0.42	0.05	0.66
psisat	Soil saturated potential	0.62	0.04	0.62
dksat	Saturated hydraulic conductivity (m/s)	1.41e−5	5e−7	3e−4
bexp	Infiltration rate parameter	4.26	2.91	10.8
nroot	Number of soil layers containing vegetation roots	3	0	4
rsmin	Minimum stomatal resistance (m)	100	40	1000
rgl	Canopy resistance/solar radiation parameter	100	30	150
hs	Canopy resistance/vapor pressure deficit parameter (s/m)	42	36.35	55
z0	NOAH surface roughness correlation length (m)	0.011	0.01	0.99
lai	Leaf-area index	4	0.05	6

begin simulation on May 30th, 2004. Soil moisture evolution is modeled over a period of 99 days through September 6th and calibration statistics consider model performance over this period.

2.3. The likelihood speckle model

The exponential speckle model defined by

$$P(I|\sigma) = \frac{1}{\sigma} \times \exp\left(\frac{-I}{\sigma}\right) \quad (6)$$

$$I = \sigma \times n \quad (7)$$

$$P(n) = \exp(-n) \quad (8)$$

where I is measured backscatter intensity (unitless), σ is mean, or 'non-speckled', intensity, and n (unitless) is the speckle contribution is a theoretically based stochastic description of speckle effects over a static and homogeneous distributed target. The number of discrete scatterers within a resolution cell and the effect of each scatterer on the intensity of the backscatter signal are random variables (Goodman, 1975; Oliver & Quegan, 1998 pp. 96). Since soil moisture changes rapidly compared to repeat satellite overpasses, the information carrying term, σ becomes time dependent and Eq. (6) is more accurately expressed as

$$P(I_t|\sigma_t) = \frac{1}{\sigma_t} \times \exp\left(\frac{-I_t}{\sigma_t}\right). \quad (9)$$

However, because this model holds for all σ and I related by Eq. (7) and n according to Eq. (8), and assuming that all observations are independently speckled, then for T images of a homogenous area each consisting of q pixels, $\Sigma = \{\sigma_t | 1 \leq t \leq T\}$, $\mathbf{I} = \{I_{j,t} | 1 \leq j \leq q, 1 \leq t \leq T\}$, and

$$L(\Sigma|\mathbf{I}) = \prod_{t=1}^T \prod_{j=1}^q \left(\frac{1}{\sigma_t}\right) \exp\left(\frac{-I_{j,t}}{\sigma_t}\right) \quad (10)$$

Eq. (10) functions as a relative likelihood estimator for a given non-speckled backscatter intensity time series $\Sigma = \{\sigma_t\}$ given speckled observations $\mathbf{I} = \{I_{j,t}\}$. Since the AIEM (by way of HPE) can produce theoretical non-speckled backscatter intensities based on surface parameters and soil moisture and SAR imagery provides intensity observations, Eq. (10) will give the relative likelihood of any soil moisture time series provided a set of SAR images as long as AIEM parameters are known.

2.4. Calibration methods

Objective function minimization can be achieved using Shuffled Complex Evolution (SCE-UA; Duan et al., 1992, 1993). In order for such a search algorithm to work within a finite time frame, it is necessary to designate the parameter space by prescribing limits on

allowable parameter values. Reasonable NOAH parameters are given by Hogue et al. (2005) (Table 1, columns 4 and 5), and the valid range for IEM surface roughness parameters is $h_{rms} < \frac{2\lambda}{2\pi}$ where λ is the wavelength (Su et al., 1997; Baghdadi & Zribi, 2006).

2.4.1. Multilook calibration (control)

Multilook methods for calibrating an LSM to SAR imagery require estimating a soil moisture time series over a given land area from imagery, and subsequently calibrating LSM parameters by comparing modeled and derived soil moisture estimates (e.g. Santanello et al., 2007). The AIEM and HPE can be inverted to estimate VWC from imagery by creating a look-up table indexed by mean backscatter intensity. NOAH parameters are estimated by reducing a MSE objective function between these image-derived values, and model output resulting in a calibrated soil moisture time series (Fig. 2a). Because soil moisture must be directly estimated from imagery using the AIEM model it is necessary to know values for the surface roughness parameters h_{rms} and C_L . These parameters can be estimated along with NOAH parameters by creating a new AIEM look-up table during each SCE-UA search iteration. Calibration then involves evaluation of an objective function comparing two modeled values, both dependent on flexible parameters. Results of implementing this algorithm are presented later, however a subjective analysis of the objective function space relative to important NOAH and AIEM parameters, for instance variable along the h_{rms} and maximum VWC (*smcmax*) parameter dimensions (Fig. 3a), reveals that this search is a somewhat of an ill-posed problem. Alternatively, surface roughness parameters can be inferred from imagery and assigned a priori. When using such parameterizations to estimate soil moisture with the AIEM it is necessary to assume that a single soil moisture value and single surface roughness values represent a multi-pixel homogenous area. Backscatter intensity is averaged over the given pixels to account for speckle and h_{rms} and C_L values are inferred using the method of Rahman et al. (2008). When this is done the LSM model output is compared to the multilook-derived representative value using a MSE objective function.

2.4.2. Likelihood calibration (experimental)

The NOAH land surface model will report a soil moisture time series, $\Phi = \{\phi_t | \forall t\}$, according to a supplied set of land surface parameters (θ), which can then be translated into modeled backscatter estimates $\Sigma = \{\sigma_t | \forall t\}$ using the AIEM and HPE. Parameters for the NOAH and AIEM models can be estimated simultaneously using Eq. (10) as the objective function noting that model parameters map uniquely to soil moisture in NOAH and soil moisture maps uniquely (given a parameter set) to backscatter through the AIEM. Effectively, the NOAH, HPE and AIEM model implemented in series can be thought of as a single LSM outputting theoretical non-speckled backscatter operating on a shared parameter set (Fig. 2b). This formulation allows AIEM surface roughness parameters to be calibrated in batch with NOAH LSM parameters using an objective

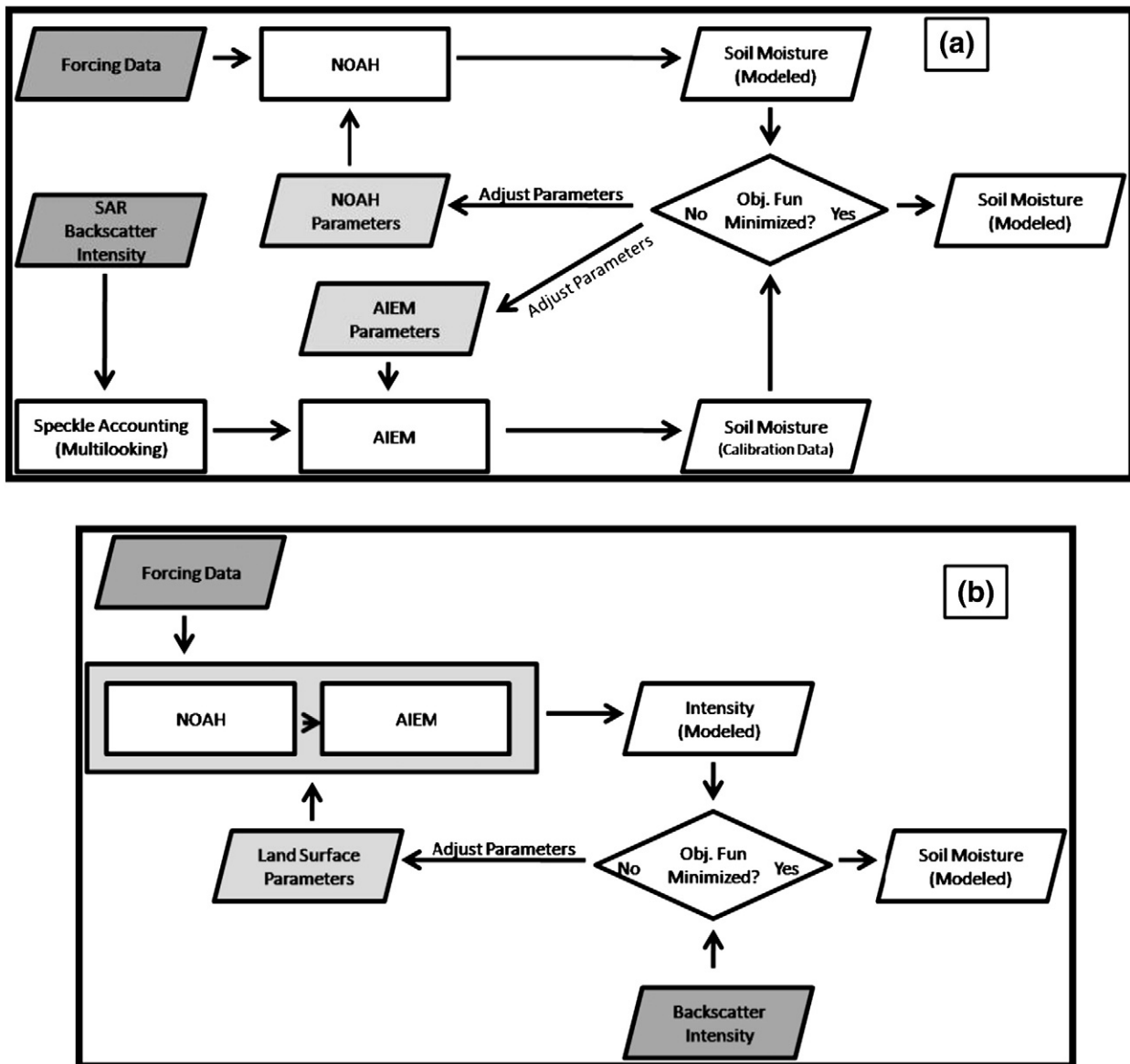


Fig. 2. Flowchart of (a) the multilook calibration algorithm with option to estimate AIEM parameters, and (b) the likelihood calibration algorithm with estimated AIEM parameters.

function which compares modeled to observed values, resulting in objective function space which is less noisy than that of the similar multilook MSE calibration method (Fig. 3b).

Maximizing the likelihood measure expressed by Eq. (10) is done by minimizing the negative of the log likelihood objective function,

$$\ln(L(M(\theta) | I)) = \ln(L(I)) \propto \sum_{t=1}^T \sum_{j=1}^q \ln\left(\left(\frac{1}{\sigma_t}\right) \exp\left(\frac{-I_{j,t}}{\sigma_t}\right)\right), \quad (11)$$

with respect to model parameters (θ).

2.5. Study site and SAR imagery

Model simulations are conducted using forcing data from the Walnut Gulch Experimental Watershed (WGEW) in southeastern Arizona. The Kendall observation site (latitude: 31.7365, longitude: -109.9419) is instrumented with a micro-meteorological flux station which provides the atmospheric measurements needed to run NOAH at 20-minute time steps. In addition, Stevens Hydra-Probe dielectric soil moisture sensors located at 5, 15, and 30 cm below the soil surface provide accurate in situ

soil moisture information recorded at the same time intervals as the atmospheric data. The history of instrumentation (Keefer et al., 2008) provides enough forcing data to initialize the land surface model. Historical data records for the WGEW are made available through the USDA-ARS Southwest Watershed Research Center's data access project (Nichols & Anson, 2008).

Current with SAR images, land cover at the site is characterized by 15–50% bare soil, 15–55% rock, 20–45% litter and 5–15% plant crown (Skirvin et al., 2008). It has been demonstrated that this amount of vegetation at the site does not significantly affect SAR retrieval of soil moisture information (Moran et al., 2000). The soil is a gravelly sandy-loam mixture (Osterkamp, 2008) which dries out quickly in the absence of precipitation.

Much of the average 312 mm of annual precipitation at the WGEW occurs as part of the summer monsoons in July and August with a smaller but significant portion occurring during the winter months of December through March (Goodrich et al., 2008). It is quite common for the soil to reach a desiccated state during the dry summer months of April, May and June further negating any effects of poor model initialization when a model spin-up period includes the summer months.

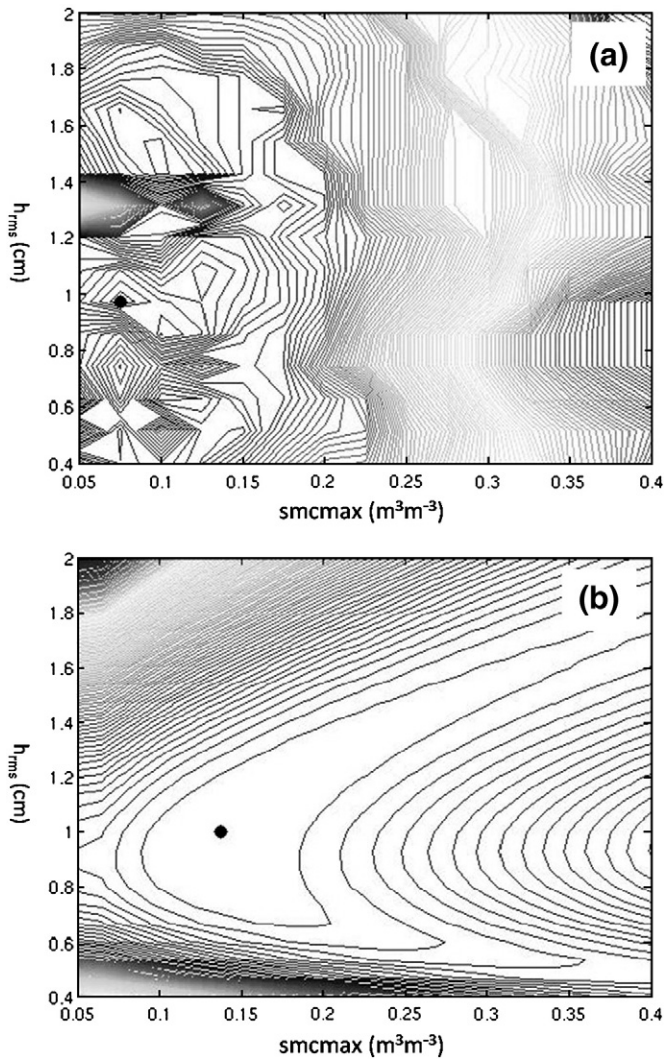


Fig. 3. (a) Multilook MSE and (b) likelihood objective function space topographies considering NOAH maximum volumetric water content ($smcmax$) and AIEM surface roughness root mean square height (h_{rms}). The black marker represents the minimum objective function value found using a grid search.

Images providing calibration observations were taken by the European Space Agency's ENVISAT-ASAR (ENVIRONMENT SATellite – Advanced Synthetic Aperture Radar) instrument and the Canadian Space Agency's Radarsat, both operating in the C band (5.6 GHz). Three ENVISAT and three Radarsat images are used spanning the dates of June 9th, 2004 to Aug 16th, 2004 (Table 2). The images are obtained with three looks and have a square pixel size of 12.5×12.5 m. The ENVISAT images are VV polarized and the Radarsat images are HH polarized. This image set has information about both dry and wet soil moisture periods and thus provides relatively good model calibration information given the inherent limitation on collection frequency (see Sorooshian et al., 1983).

Table 2
SAR image parameters.

Date	Time	Instrument	Pixel dimension	Incidence angle	Wavelength	Polarization
June 9	10:16	ENVISAT	12.5 m	41.08°	5.6 cm	VV
July 14	10:16	ENVISAT	12.5 m	41.08°	5.6 cm	VV
Aug 2	10:16	ENVISAT	12.5 m	37.39°	5.6 cm	VV
Aug 6	18:20	RADARSAT	12.5 m	35.93°	5.6 cm	HH
Aug 16	18:20	RADARSAT	12.5 m	46.48°	5.6 cm	HH
Aug 20	18:20	RADARSAT	12.5 m	46.48°	5.6 cm	HH

2.6. Simulated data tests

Parameter uncertainty, model structural error, and observation error contribute to uncertainty in model simulations. Calibration procedures, in general, attempt to account for model parameter uncertainty, and it is important to understand the effects of other potential sources. To this end parameters are first calibrated using simulated imagery in a way which eliminates effects of both NOAH and AIEM structural error on the modeled soil moisture output. A NOAH soil moisture time series considered the true state, created using a known land surface parameter set and measured atmospheric forcing data, is used to generate 7×7 pixel simulated SAR backscatter intensity images by assigning values to AIEM surface roughness parameters and using the HPE and AIEM to convert the simulated soil moisture to backscatter intensity. Surface roughness parameters values of $h_{rms} = 1.48$ cm and $C_L = 1.25$ cm used for this procedure are chosen using the SCE-UA to minimize the MSE between measured and modeled backscatter assuming that NOAH VWC time series calibrated to in situ measurements is correct. These values represent our best guess as to the surface roughness characterization which will elicit optimal behavior in the AIEM over this area according to the real SAR imagery which is available. Speckle is simulated by adding noise according to Eqs. (7) and (8). NOAH parameters (and in some cases AIEM h_{rms} and C_L) are then back-estimated by employing the likelihood and multilook calibration methods.

When surface roughness is assumed a priori, h_{rms} and C_L are chosen to be the actual values used to create the simulated imagery with the addition of simulated measurement error as a percentage of the true value ranging from 0 to 20%. Different measurement techniques (instrument, transect length, algorithm, etc.) for determining h_{rms} and C_L can result in different parameter values (Mattia et al., 2003; Bryant et al., 2007; Rahman et al., 2008) such that, often, measurements are not useable for accurate soil moisture inversion. The effect of this simulated measurement error is demonstrated using a series of 10 simulated images as system observations. Alternatively, surface roughness is calibrated along with NOAH parameters. Both procedures, one assuming a priori surface roughness parameters and the other attempting to calibrate them, are performed using the multilook and likelihood approaches with identical sets of simulated imagery as observations.

2.7. Real data tests

Secondly, NOAH is calibrated using in situ measurements of soil moisture and validated against the observation data set, a procedure which will be influenced by model structural errors but not as significantly by system observation errors since the observation data are also the validation data and are assumed to represent the true soil moisture states. Similarly, parameter estimation using the portion of the in situ data corresponding to SAR overpass times demonstrates the maximum potential for using a sparse soil moisture observation set, such as one derived from satellite imagery, in absence of speckle or AIEM uncertainty.

Finally, the proposed likelihood method is applied to estimate NOAH and AIEM parameters using SAR imagery and validated against the in situ data set. The performance of this procedure is compared to

that of the multilook procedures with MSE objective functions, again assuming both known and calibrated surface roughness. Roughness parameters assumed a priori have average values over the 7×7 pixel area of $h_{rms} = 0.57$ cm, and $C_t = 0.76$ cm found using the method of Rahman et al. (2008). VWC thus derived from each image are given in Table 4.

In order to infer soil moisture it is necessary to assume that an area of some size is homogenous. Moisture estimates are derived for image squares of 5×5 , 7×7 , 9×9 , 11×11 , 15×15 , and 21×21 pixels, representing aggregated land areas both above and below the 8×8 SAR pixel (100 m \times 100 m) limitation imposed by product requirements. Performance statistics are computed comparing the modeled soil moisture value representative of the land surface area to the point-based in situ measured soil moisture at 5 cm depth.

3. Results

3.1. Comparing simulated data tests

When applied in the absence of model structural error the likelihood objective function calibration consistently out-performs the multilook-derived soil moisture calibration in ability to parameterize the model with the goal of estimating surface level soil moisture between satellite overpasses. When AEM surface roughness is assumed a priori the likelihood approach is able to extract soil moisture time correlation information from the land surface model to improve speckle accounting; the effect of any particular speckled pixel is reduced due to the increase in sample size by sampling through time. This ability diminishes as the accuracy of the a priori surface roughness degrades, most likely due to the fact that the AEM is highly sensitive to surface roughness, and other factors affecting calibrated model error quickly become dominated by surface roughness parameterization error (Fig. 4). Additionally, the likelihood objective function space allows for a more functional estimation of AEM parameters in batch with NOAH parameters. However, neither method is able to consistently estimate the actual parameter values used to create the model-generated VWC series (Fig. 5). At times the difference between calibrated and actual values could be as much as 70% of the allowable parameter range. Because many different parameter sets will result in relatively similar model outputs – a phenomenon encountered in hydrologic modeling known as equifinality (Beven & Binley, 1992; Beven, 2006) – small changes in calibration data measurements can result in drastic changes to calibrated parameter values.

3.2. Comparing real data tests

The ability of the model to represent the in situ observations can be seen in Fig. 6b. Given this optimal calibration, NOAH predicts with 95% confidence of ± 0.02 [m^3/m^3]. Reduction in the calibration data density from continuous to on the order of SAR revisit frequency (Fig. 6d) results in a 95% prediction confidence of ± 0.03 [m^3/m^3] (Table 3). Visual inspection of the VWC time series also suggests that both the full and sparse data sets offer enough information to facilitate reliable predictions in most cases, however peak soil moisture is over predicted using the sparse set since there are no observations of peak behavior.

Parameter estimation using imagery clearly demonstrates the importance of accounting for uncertainty in SAR measurements of soil moisture. With observations consisting of square 7×7 pixel images the multilook method with a priori surface roughness resulted in substantial disagreement and bias, predicting with 95% confidence to within ± 0.10 [m^3/m^3]. Likelihood calibration offers error and bias improvement with, in this case, a 95% confidence interval of ± 0.04 [m^3/m^3] VWC and a reduction in absolute residuals bias (Table 3, Fig. 6). Again, the reasons for improvement are twofold: the effect of any particular significantly speckled radar pixel is reduced in the likelihood algorithm due to the

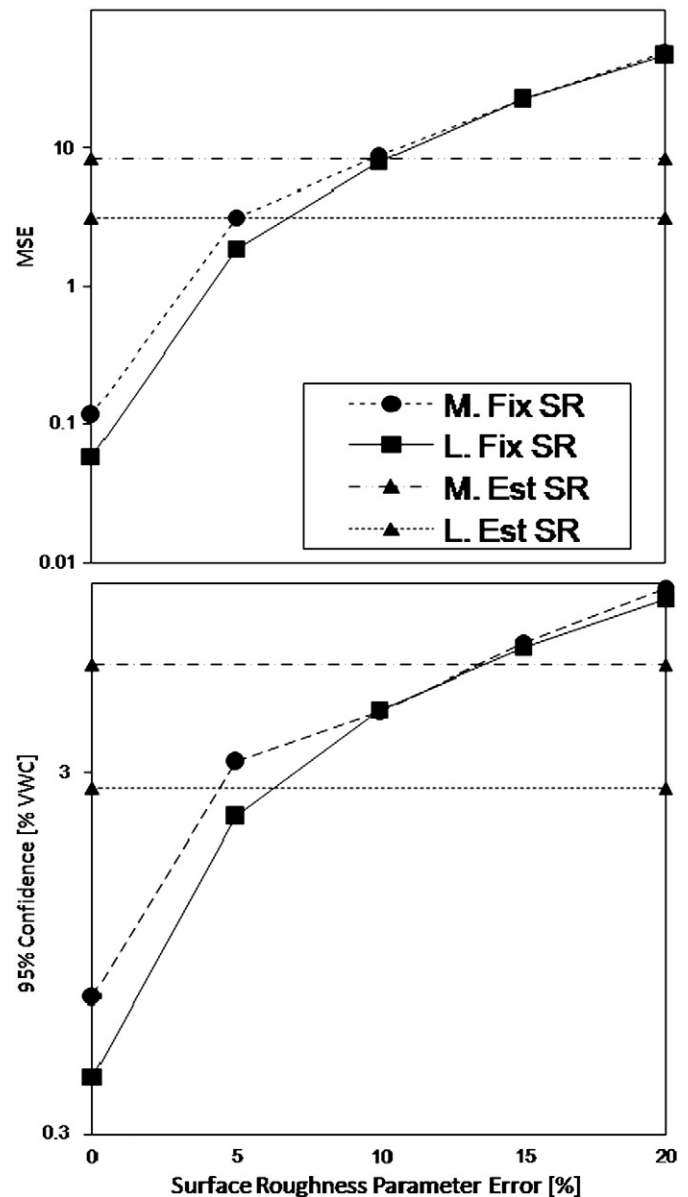


Fig. 4. (*M. Fix SR*) Multilook and (*L. Fix SR*) likelihood calibration sensitivity to fixed a priori AEM surface roughness parameter error compared to (*Est SR*) estimating these parameters – 10 7×7 pixel simulated images are used as observations.

increase in sample size by sampling through time, and the likelihood objective function formulation is better suited for calibrating surface roughness parameters in batch with LSM parameters. Soil moisture derived using multilook methods and modeled by a calibrated LSM are reported in Table 4 along with the estimated surface roughness parameters. VWC inferred from the HH polarized imagery using a priori roughness are high (due to poorly estimated representative surface roughness values) compared to in situ measurements resulting in substantially biased model predictions.

3.3. The effects of the homogeneity assumption

The usability of either method is heavily dependent on the assumption that a given land surface area is homogeneous in terms of roughness and moisture characteristics. While it is possible to derive soil moisture estimates from SAR imagery under this assumption (e.g. Thoma et al., 2008), these estimates are an effective value for the aggregated area. Both the characteristics of the land surface itself and speckle accounting requirements will determine the effects of the homogeneity assumption

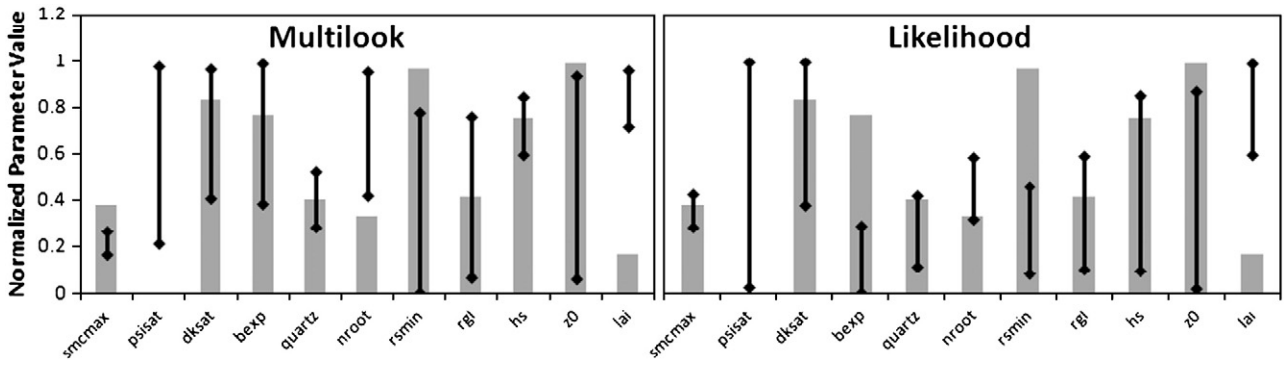


Fig. 5. Normalized actual parameter values (histograms), and normalized calibrated parameter range (black bars) over 5 trials using 10 simulated 7 × 7 pixel images.

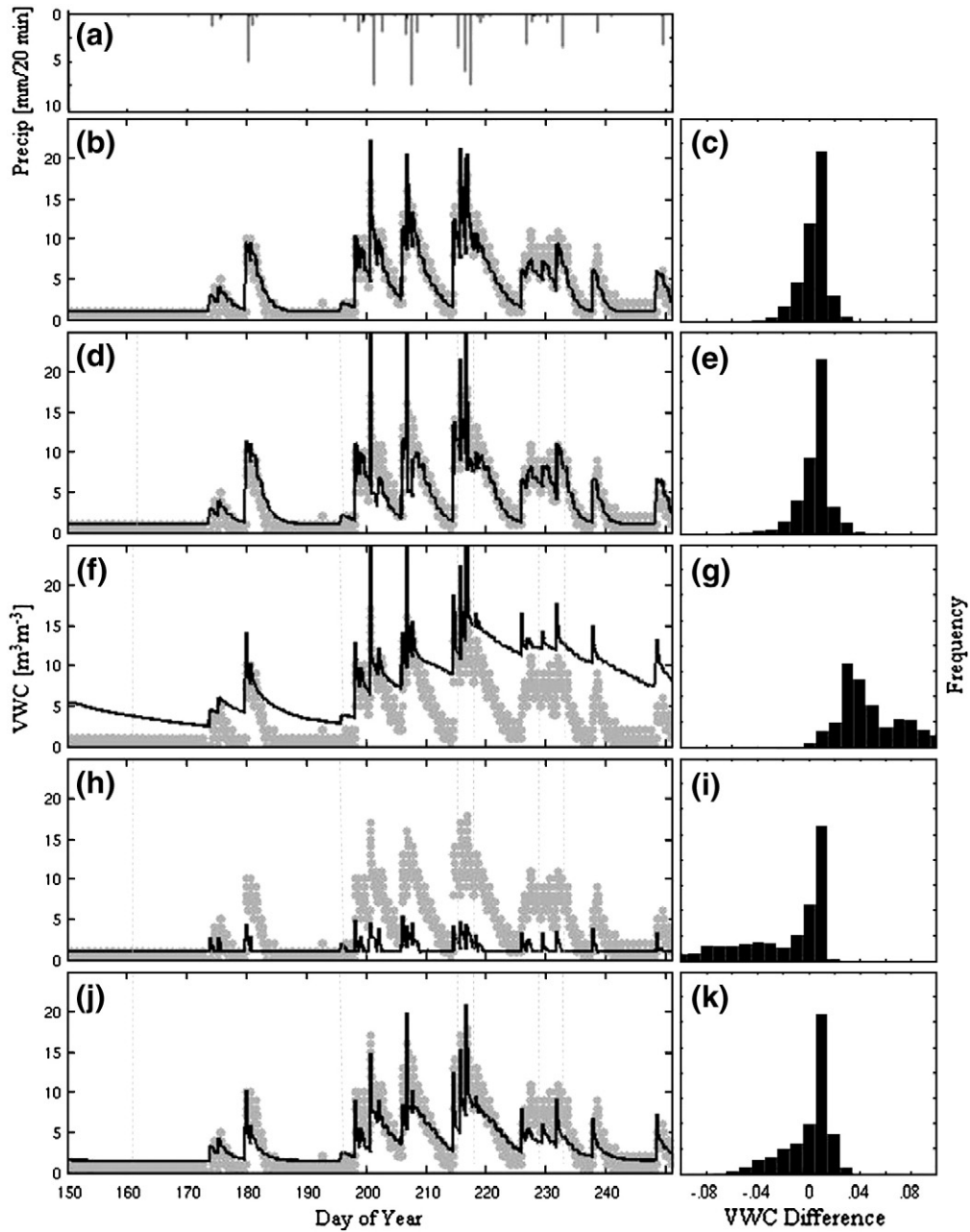


Fig. 6. (a) Simulation period precipitation and NOAH calibrated soil moisture time series and residuals using (b,c) in situ measurements (gray dots on all) as system observations, (d, e) in situ measurements taken at times of SAR imagery, (f,g) SAR imagery and multilook calibration with Rahman et al. (2008) surface roughness parameters, (h,i) multilook calibration with estimated surface roughness, and (j,k) likelihood calibration. Dotted gray lines represent SAR image times.

Table 3
Performance statistics for multilook and likelihood surface-level soil moisture calibration attempts using 7×7 pixel SAR imagery as system observations. Statistics represent a comparison between modeled and in situ measured soil moisture at all 20-minute time steps over the 99-day simulation period.

	In-situ calibration		SAR calibration (7×7 pixels)		
	Continuous	Sparse	Multilook fixed SR	Multilook est. SR	Likelihood
95% confidence [m ³ /m ³]	0.02	0.03	0.10	0.08	0.04
Mean squared error	1.45	2.83	28.17	14.56	4.79
Residual percent bias [m ³ /m ³ *100]	13.87	14.28	155.15	-59.82	10.82

on spatial resolution and accuracy, this study only looks at the effect of radar pixel sample size.

Fig. 7 suggests that calibrated model prediction capability improves as the land surface area considered increases until the homogeneity assumption begins to fail. As the pixel sample size taken from individual images increases speckle accounting improves on average, resulting in more accurate observation data and calibrated time series, however as the area increases the point-based in situ measurements may not well represent the imaged land surface. An examination of (Table 4) values of image-derived moisture estimates indicates that AIEM error affects the multilook calibration suggesting that the image method for deriving surface roughness is unreliable at these scales. Because speckle influences the per-pixel surface roughness estimates using the image-based a priori method, the image-derived surface roughness parameters better represent the imaged area on average as the sample size increases. As an example, an area of 11×11 pixels report surface roughness parameter values of $C_L = 1.20$ cm and $h_{rms} = 0.71$ cm compared to values of $C_L = 0.76$ cm and $h_{rms} = 0.57$ cm when an area of 7×7 is used. In the former case soil moisture is inferred from imagery at the reported times (Table 2) as 1, 1, 2, 4, 6, 6 (% VWC) and in the latter as 4, 3, 6, 12, 15, 15 (% VWC); inaccurate roughness parameters are detrimental to the calibration effort – neither of these estimates match well the in situ measurements of 1, 2, 11, 8, 8, 3 (% VWC).

The multilook algorithm estimating surface roughness is relatively consistent in terms of accuracy independent of sample size, which is explained by noting (not shown) that this algorithm finds maximum agreement between NOAA modeled soil moisture and AIEM (with HPE)

Table 4
Soil moisture and surface roughness parameters measured in situ and derived using calibration methods and real SAR images of a 7×7 pixel area. Likelihood calibration does not derive a soil moisture value from imagery directly, the derived values reported here are found with an AIEM and HPE look-up table using the estimated values of surface roughness parameters. Calibrated surface roughness values in the in situ column represent values found by first calibrating NOAA to in situ soil moisture measurements and then estimating AIEM surface roughness parameters using SAR imagery as observations and an MSE objective function between modeled and measured backscatter.

	In situ		Multilook fixed SR		Multilook est. SR		Likelihood	
	Measured	Derived	Modeled	Derived	Modeled	Derived	Modeled	
Image-derived and modeled soil moisture [% VWC]								
June 9	0	4	3.7	1	1.0	1	1.5	
July 14	2	3	3.8	1	1.2	1	2.3	
Aug 2	11	6	11.3	1	1.6	4	5.5	
Aug 6	8	12	14.1	1	1.0	6	7.0	
Aug 16	8	15	12.8	1	1.3	6	5.1	
Aug 20	3	15	11.3	1	1.0	6	3.4	
Surface roughness parameters [cm]								
	Calibrated		Measured		Calibrated		Calibrated	
h_{rms}	1.48		0.57		1.21		2.55	
C_L	1.25		0.76		3.21		2.73	

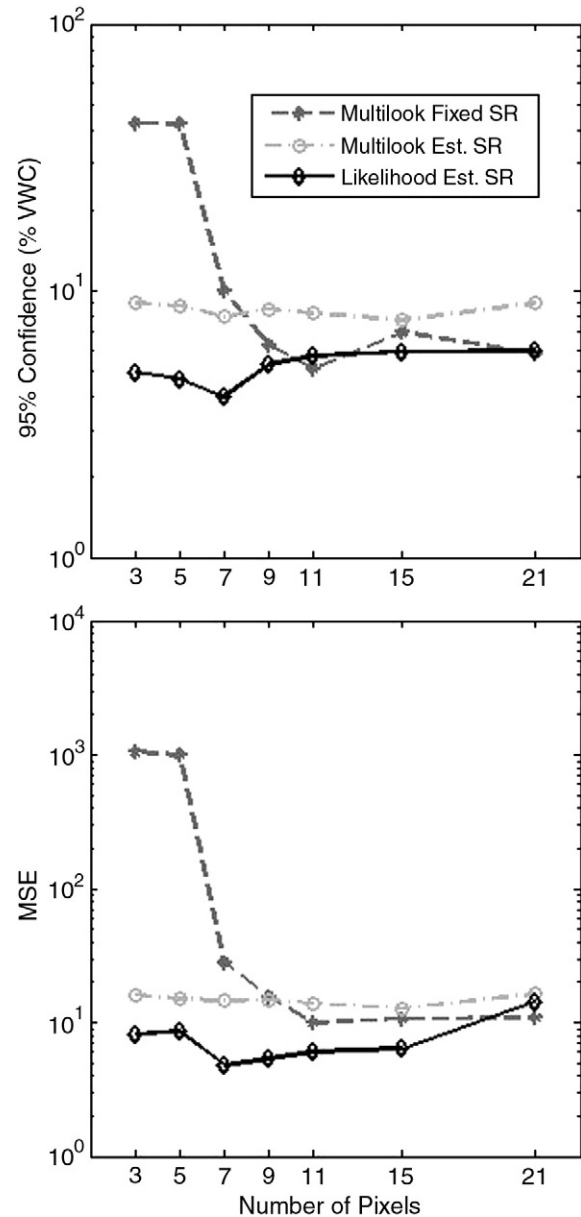


Fig. 7. Performance statistics (top) 95% prediction confidence and (bottom) mean squared error (MSE) between calibrated model generated surface level soil moisture and in situ measurements (5 cm depth) using SAR imagery as observations. X-axis labels represent the square-side number of image pixels sampled as homogeneous. Performance statistics are derived over the entire 99 day validation period.

inverted soil moisture when parameters are chosen such that the two models both report very low VWC values – almost consistently at the allowed minimum of 1%. An example of this can be seen in Fig. 6h as part of the real data trial.

4. Discussion on the handling of uncertainty

Land surface models are effective in estimating a state variable if (i) they are appropriately parameterized, (ii) model structure is sufficiently accurate and robust, and (iii) the forcing data (such as precipitation) is sufficiently accurate. Although a demonstration of the ability of the LSM to match observations is given, model structural uncertainty is not explicitly accounted for in any calibration algorithm presented here. Perhaps as importantly, calibration generally does not

consider inaccurate or uncertain forcing data. Calibration is a process of accounting for model parameter uncertainty, and in this case we also show that some marginal benefit to speckle accounting can be obtained using the likelihood objective function. In fact, likelihood calibration implicitly estimates the information carrying parameters ($\{\sigma_i\}$) from a traditional likelihood speckle accounting scheme. On the other hand, data assimilation studies often seek to account for forcing data (usually precipitation) deficiencies by merging (soil moisture) observations with model state estimates (e.g. Crow & Wood, 2003; Reichle & Koster, 2005; Crow, 2007). As it stands, the calibration mechanisms presented here would not allow for simultaneous attenuation of the effects of forcing data and parameter uncertainty; merging calibration and assimilation activities is an active area of research (e.g. Vrugt et al., 2005).

In general, the ability to map soil moisture with radar imagery is dependent on the accuracy of the backscatter inversion technique. In this case the AIEM is chosen because of its prevalence (Moran et al., 2004; Verhoest et al., 2008), however it has been reported that the IEM may not be an accurate representation of the backscattering behavior of real land surfaces (e.g. Rakotoarivony et al., 1996; Zribi et al., 1997; Baghdadi et al., 2004, 2006). Verhoest et al. (2008) proposes that this is due to (i) intra-field heterogeneity in terms of roughness and moisture conditions, (ii) the fact that volumetric scattering from the sub-surface is neglected, and (iii) that assumptions implicit in the model structure may be incorrect (the validity of assumptions is unverified). Unfortunately because of speckle, estimating dielectric properties from imagery requires a homogeneity assumption, the hope being that when the model is inverted representative values of surface roughness parameters for the area and model structure are sufficient for inferring representative dielectric properties, and thus water content. This assumption will neglect any interacting effects between backscatter from intra-area heterogeneities which are not accounted for in the parameterization such as multi-scale roughness patterns (Mattia & Le Toan, 1999). We find in all cases described here that the retrieval of soil moisture through inversion of the AIEM are subject to some substantial error and should be treated as uncertain and imprecise. Partly because it is often difficult to accurately infer soil moisture from SAR imagery, data assimilation studies will sometimes focus on inferring climatological anomalies by merging models and imagery rather than attempt to extract precise VWC measurements (Bolten et al., 2009; Crow, 2007).

Because of the sensitivity of calibration results to surface roughness parameterization the importance of AIEM parameter uncertainty must be emphasized. The likelihood method chooses surface roughness parameter values which do not result in large disagreements between soil moisture derived from different images that cannot be explained by the model forcing data and structure. Although likelihood calibration does offer some improvement in speckle accounting for the purposes of calibrating a LSM (Fig. 4), it is apparent from comparing the values of soil moisture inferred from imagery and calibration that differences in surface roughness parameterization plays a significant role in the determining calibrated model response (compare Table 4 and Fig. 6). It is apparent, however, that even this method of parameterizing the AIEM is probably not optimal, as VWC derived from imagery using the estimated parameter value does not agree well with in-situ measurements.

5. Conclusion

This paper outlines an approach to mapping distributed surface level soil moisture between satellite overpasses using land surface models calibrated with SAR imagery based on maximum likelihood speckle accounting. The method is demonstrated using the NOAA land surface model and the Advanced Integral Equation Method backscatter model to invert soil dielectric properties. Likelihood calibration is tested using simulated imagery, demonstrating marginal improvement over strict multilooking methods for speckle accounting, and with real imagery of a

location in the southwestern United States demonstrating improvement in agreement with point-based in situ measurements at small scales. Improvement is due mostly to the algorithm's ability to estimate AIEM surface roughness parameter values which are functional in terms of deriving soil moisture over the set of available images. Effects of AIEM surface roughness parameter uncertainty on model output show that calibration is especially sensitive to these surface roughness parameter values, which is consistent with previous studies. Investigation of the effects of assuming homogeneity over an imaged area reveals that the AIEM has value in terms of deriving descriptive parameter sets for distributed areas, although this ability diminishes if the area is too large to be considered homogeneous or too small for speckle accounting.

Acknowledgements

The authors would like to thank Tom Jackson at the USDA-ARS Hydrology and Remote Sensing Lab for providing ENVISAT imagery, as well as Magfur Rahman with Saskatchewan Environment and Resource Management for providing Radarsat imagery and algorithms.

References

- Altese, E., Bolognani, O., Mancini, M., & Troch, P. A. (1996). Retrieving soil moisture over bare soil from ERS 1 synthetic aperture radar data: Sensitivity analysis based on a theoretical surface scattering model and field data. *Water Resources Research*, 32, 653–661.
- Baghdadi, N., Gaultier, S., & King, C. (2002a). Retrieving surface roughness and soil moisture from synthetic aperture radar (SAR) data using neural networks. *Canadian Journal of Remote Sensing*, 28, 701–711.
- Baghdadi, N., Gherboudj, I., Zribi, M., Sahebi, M., King, C., & Bonn, F. (2004). Semi-empirical calibration of the IEM backscattering model using radar images and moisture and roughness field measurements. *International Journal of Remote Sensing*, 25, 3593–3623.
- Baghdadi, N., Holah, N., & Zribi, M. (2006). Calibration of the integral equation model for SAR data in C-band and HH and VV polarizations. *International Journal of Remote Sensing*, 27, 805–816.
- Baghdadi, N., King, C., Bourguignon, A., & Remond, A. (2002b). Potential of ERS and Radarsat data for surface roughness monitoring over bare agricultural fields: Application to catchments in Northern France. *International Journal of Remote Sensing*, 23, 3427–3442.
- Baghdadi, N., Paillou, P., Grandjean, G., Dubois, P., & Davidson, M. (2000). Relationship between profile length and roughness variables for natural surfaces. *International Journal of Remote Sensing*, 21, 3375–3381.
- Baghdadi, N., & Zribi, M. (2006). Evaluation of radar backscatter models IEM, OH and Dubois using experimental observations. *International Journal of Remote Sensing*, 27, 3831–3852.
- Beven, K. (2006). A manifesto for the equifinality thesis. *Journal of Hydrology*, 320, 18–36.
- Beven, K., & Binley, A. (1992). The future of distributed models – Model calibration and uncertainty prediction. *Hydrological Processes*, 6, 279–298.
- Bolten, J. D., Crow, W. T., Zhan, X., Reynolds, C. A., & Jackson, T. J. (2009). Assimilation of a satellite-based soil moisture product into a two-layer water balance model for a global crop production decision support system. In S. K. Park, & L. Xu (Eds.), *Data assimilation for atmospheric, oceanic and hydrologic applications* (pp. 449–463). Berlin: Springer-Verlag.
- Bryant, R., Moran, M. S., Thoma, D. P., Collins, C. D. H., Skirvin, S., Rahman, M., et al. (2007). Measuring surface roughness height to parameterize radar backscatter models for retrieval of surface soil moisture. *IEEE Geoscience and Remote Sensing Letters*, 4, 137–141.
- Burke, E. J., Gurney, R. J., Simmonds, L. P., & Jackson, T. J. (1997). Calibrating a soil water and energy budget model with remotely sensed data to obtain quantitative information about the soil. *Water Resources Research*, 33, 1689–1697.
- Calvet, J. C., & Noilhan, J. (2000). From near-surface to root-zone soil moisture using year-round data. *Journal of Hydrometeorology*, 1, 393–411.
- Chen, K. S., Wu, T. D., Tsang, L., Li, Q., Shi, J. C., & Fung, A. K. (2003). Emission of rough surfaces calculated by the integral equation method with comparison to three-dimensional moment method simulations. *IEEE Transactions on Geoscience and Remote Sensing*, 41, 90–101.
- Crow, W. T. (2007). A novel method for quantifying value in spaceborne soil moisture retrievals. *Journal of Hydrometeorology*, 8, 56–67.
- Crow, W. T., & Wood, E. F. (2003). The assimilation of remotely sensed soil brightness temperature imagery into a land surface model using ensemble Kalman filtering: A case study based on ESTAR measurements during SGP97. *Advances in Water Resources*, 26, 137–149.
- Diskin, M. H., & Simon, E. (1977). Procedure for selection of objective functions for hydrologic simulation models. *Journal of Hydrology*, 34, 129–149.
- Dobson, M. C., Ulaby, F. T., Hallikainen, M. T., & Elrayes, M. A. (1985). Microwave dielectric behavior of wet soil. 2. Dielectric mixing models. *IEEE Transactions on Geoscience and Remote Sensing*, 23, 35–46.

- Duan, Q. Y., Gupta, V. K., & Sorooshian, S. (1993). Shuffled complex evolution approach for effective and efficient global minimization. *Journal of Optimization Theory and Applications*, 76, 501–521.
- Duan, Q. Y., Sorooshian, S., & Gupta, V. (1992). Effective and efficient global optimization for conceptual rainfall-runoff models. *Water Resources Research*, 28, 1015–1031.
- Ek, M. B., Mitchell, K. E., Lin, Y., Rogers, E., Grunmann, P., Koren, V., et al. (2003). Implementation of Noah land surface model advances in the National Centers for Environmental Prediction operational mesoscale Eta model. *Journal of Geophysical Research-Atmospheres*, 108, 8851, doi:10.1029/2002JD003296.
- Feddes, R. A., Menenti, M., Kabat, P., & Bastiaanssen, W. G. M. (1993). Is large-scale inverse modeling of unsaturated flow with areal average evaporation and surface soil-moisture as estimated from remote sensing feasible. *Journal of Hydrology*, 143, 125–152.
- Fung, A. K., Dawson, M. S., Chen, K. S., Hsu, A. Y., Engman, E. T., O'Neill, P. E., et al. (1996). A modified IEM model for scattering from soil surfaces with application to soil moisture sensing. *Proceedings of the International Geoscience and Remote Sensing Symposium (IGARSS'96), Lincoln, Nebraska, USA* (pp. 1297–1299).
- Fung, A. K., Li, Z. Q., & Chen, K. S. (1992). Backscattering from a randomly rough dielectric surface. *IEEE Transactions on Geoscience and Remote Sensing*, 30, 356–369.
- Goodman, J. W. (1975). Statistical properties of laser speckle patterns. In J. C. Dainty (Ed.), *Topics in applied physics. Laser speckle and related phenomena*, 9. (pp. 19–75) Berlin: Springer-Verlag.
- Goodrich, D. C., Keefer, T. O., Unkrich, C. L., Nichols, M. H., Osborn, H. B., Stone, J. J., et al. (2008). Long-term precipitation database, Walnut Gulch Experimental Watershed, Arizona, United States. *Water Resources Research*, 44, W05S04, doi:10.1029/2006WR005782.
- Gutman, G., & Ignatov, A. (1998). The derivation of the green vegetation fraction from NOAA/AVHRR data for use in numerical weather prediction models. *International Journal of Remote Sensing*, 19, 1533–1543.
- Hallikainen, M. T., Ulaby, F. T., Dobson, M. C., Elrayes, M. A., & Wu, L. K. (1985). Microwave dielectric behavior of wet soil. 1. Empirical models and experimental observations. *IEEE Transactions on Geoscience and Remote Sensing*, 23, 25–34.
- Hogue, T. S., Bastidas, L., Gupta, H., Sorooshian, S., Mitchell, K., & Emmerich, W. (2005). Evaluation and transferability of the Noah land surface model in semiarid environments. *Journal of Hydrometeorology*, 6, 68–84.
- Ines, A. V. M., & Mohanty, B. P. (2008). Near-surface soil moisture assimilation for quantifying effective soil hydraulic properties using genetic algorithm: 1. Conceptual modeling. *Water Resources Research*, 44, W06422, doi:10.1029/2007WR005990.
- Ines, A. V. M., & Mohanty, B. P. (2009). Near-surface soil moisture assimilation for quantifying effective soil hydraulic properties using genetic algorithms: 2. Using airborne remote sensing during SGP97 and SMEX02. *Water Resources Research*, 45, W01408, doi:10.1029/2008WR007022.
- Jiang, L., Kogan, F.N., Guo, W., Tarpley, J.D., Mitchell, K.E., Ke, M.B., Tian, Y., Zheng, W., Zou, C., Ramsay, B. (2009). Real time weekly global green vegetation fraction derived from AVHRR-based NOAA operational global vegetation index (GVI) system. In review: *Journal of Geophysical Research – Atmospheres*.
- Johnston, P. R., & Pilgrim, D. H. (1976). Parameter optimization for watershed models. *Water Resources Research*, 12, 477–486.
- Keefer, T. O., Moran, M. S., & Paige, G. B. (2008). Long-term meteorological and soil hydrology database, Walnut Gulch Experimental Watershed, Arizona, United States. *Water Resources Research*, 44, W05S07, doi:10.1029/2006WR005702.
- Koster, R. D., Suarez, M. J., Liu, P., Jambor, U., Berg, A., Kistler, M., et al. (2004). Realistic initialization of land surface states: Impacts on subseasonal forecast skill. *Journal of Hydrometeorology*, 5, 1049–1063.
- Liu, Y. Q., & Gupta, H. V. (2007). Uncertainty in hydrologic modeling: Toward an integrated data assimilation framework. *Water Resources Research*, 43, W07401, doi:10.1029/2006WR005756.
- Mahrt, L., & Pan, H. (1984). A 2-layer model of soil hydrology. *Boundary-Layer Meteorology*, 29, 1–20.
- Mattia, F., Davidson, M. W. J., Le Toan, T., D'Haese, C. M. F., Verhoest, N. E. C., Gatti, A. M., et al. (2003). A comparison between soil roughness statistics used in surface scattering models derived from mechanical and laser profilers. *IEEE Transactions on Geoscience and Remote Sensing*, 41, 1659–1671.
- Mattia, F., & Le Toan, T. (1999). Backscattering properties of multi-scale rough surfaces. *Journal of Electromagnetic Waves and Applications*, 13, 493–527.
- Mertens, J., Stenger, R., & Barkle, G. F. (2006). Multiobjective inverse modeling for soil parameter estimation and model verification. *Vadose Zone Journal*, 5, 917–933.
- Mohanty, B. P., Shouse, P. J., Miller, D. A., & van Genuchten, M. T. (2002). Soil property database: Southern Great Plains 1997 hydrology experiment. *Water Resources Research*, 38, 1047, doi:10.1029/2000WR000076.
- Moran, M. S., Hymer, D. C., Qi, J. G., & Sano, E. E. (2000). Soil moisture evaluation using multi-temporal synthetic aperture radar (SAR) in semiarid rangeland. *Agricultural and Forest Meteorology*, 105, 69–80.
- Moran, M. S., Peters-Lidard, C. D., Watts, J. M., & McElroy, S. (2004). Estimating soil moisture at the watershed scale with satellite-based radar and land surface models. *Canadian Journal of Remote Sensing*, 30, 805–826.
- Nichols, M. H., & Anson, E. (2008). Southwest watershed research center data access project. *Water Resources Research*, 44, W05S03, doi:10.1029/2006WR005665.
- Nolan, M., & Fatland, D. R. (2003). Penetration depth as a DInSAR observable and proxy for soil moisture. *IEEE Transactions on Geoscience and Remote Sensing*, 41, 532–537.
- Oelze, M. L., Sabatier, J. M., & Raspet, R. (2003). Roughness measurements of soil surfaces by acoustic backscatter. *Soil Science Society of America Journal*, 67, 241–250.
- Oh, Y., & Hong, J. Y. (2007). Effect of surface profile length on the backscattering coefficients of bare surfaces. *IEEE Transactions on Geoscience and Remote Sensing*, 45, 632–638.
- Oliver, C., & Quegan, S. (1998). *Understanding synthetic aperture radar images*. Boston: Artech House.
- Osterkamp, W. T. (2008). Geology, soils, and geomorphology of the Walnut Gulch Experimental Watershed, Tombstone, Arizona. *Journal of the Arizona-Nevada Academy of Science*, 40, 136–154.
- Pauwels, V. R. N., Balenzano, A., Satalino, G., Skriver, H., Verhoest, N. E. C., & Mattia, F. (2009). Optimization of soil hydraulic model parameters using synthetic aperture radar data: An integrated multidisciplinary approach. *IEEE Transactions on Geoscience and Remote Sensing*, 47, 455–467.
- Peters-Lidard, C. D., Mocko, D. M., Garcia, M., Santanello, J. A., Tischler, M. A., Moran, M. S., et al. (2008). Role of precipitation uncertainty in the estimation of hydrologic soil properties using remotely sensed soil moisture in a semiarid environment. *Water Resources Research*, 44, W05S18, doi:10.1029/2007WR005884.
- Podmore, T. H., & Huggins, L. F. (1981). An automated profile meter for surface-roughness measurements. *Transactions of the ASAE*, 24, 663–665.
- Rahman, M. M., Moran, M. S., Thoma, D. P., Bryant, R., Collins, C. D. H., Jackson, T., et al. (2008). Mapping surface roughness and soil moisture using multi-angle radar imagery without ancillary data. *Remote Sensing of Environment*, 112, 391–402.
- Rakotoarivony, L., Taconet, O., VidalMadjar, D., Bellemain, P., & Benallegue, M. (1996). Radar backscattering over agricultural bare soils. *Journal of Electromagnetic Waves and Applications*, 10, 187–209.
- Reichle, R. H., & Koster, R. D. (2005). Global assimilation of satellite surface soil moisture retrievals into the NASA catchment land surface model. *Geophysical Research Letters*, 32, L02404, doi:10.1029/2004GL021700.
- Rodell, M., Houser, P. R., Berg, A. A., & Famiglietti, J. S. (2005). Evaluation of 10 methods for initializing a land surface model. *Journal of Hydrometeorology*, 6, 146–155.
- Santanello, J. A., Peters-Lidard, C. D., Garcia, M. E., Mocko, D. M., Tischler, M. A., Moran, M. S., et al. (2007). Using remotely-sensed estimates of soil moisture to infer soil texture and hydraulic properties across a semi-arid watershed. *Remote Sensing of Environment*, 110, 79–97.
- Skirvin, S., Kidwell, M., Biedenbender, S., Henley, J. P., King, D., Collins, C. H., et al. (2008). Vegetation data, Walnut Gulch Experimental Watershed, Arizona, United States. *Water Resources Research*, 44, W05S08, doi:10.1029/2006WR005724.
- Sorooshian, S., & Gupta, V. K. (1985). The analysis of structural identifiability – Theory and application to conceptual rainfall-runoff models. *Water Resources Research*, 21, 487–495.
- Sorooshian, S., Gupta, V. K., & Fulton, J. L. (1983). Evaluation of maximum-likelihood parameter estimation techniques for conceptual rainfall-runoff models – Influence of calibration data variability and length on model credibility. *Water Resources Research*, 19, 251–259.
- Su, Z., Troch, P. A., & De Troch, F. P. (1997). A method for retrieving soil moisture using active microwave data. *Physics and Chemistry of the Earth*, 22, 235–239.
- Thoma, D. P., Moran, M. S., Bryant, R., Rahman, M. M., Collins, C. D. H., Keefer, T. O., et al. (2008). Appropriate scale of soil moisture retrieval from high resolution radar imagery for bare and minimally vegetated soils. *Remote Sensing of Environment*, 112, 403–414.
- Ulaby, F. T. (1974). Radar measurement of soil-moisture content. *IEEE Transactions on Antennas and Propagation*, AP22, 257–265.
- Verhoest, N. E. C., Lievens, H., Wagner, W., Alvarez-Mozos, J., Moran, M. S., & Mattia, F. (2008). On the soil roughness parameterization problem in soil moisture retrieval of bare surfaces from synthetic aperture radar. *Sensors*, 8, 4213–4248.
- Vrugt, J. A., Diks, C. G. H., Gupta, H. V., Bouten, W., & Verstraten, J. M. (2005). Improved treatment of uncertainty in hydrologic modeling: Combining the strengths of global optimization and data assimilation. *Water Resources Research*, 41, W01017, doi:10.1029/2004WR003059.
- Yapo, P. O., Gupta, H. V., & Sorooshian, S. (1998). Multi-objective global optimization for hydrologic models. *Journal of Hydrology*, 204, 83–97.
- Zribi, M., & Dechambre, M. (2003). A new empirical model to retrieve soil moisture and roughness from C-band radar data. *Remote Sensing of Environment*, 84, 42–52.
- Zribi, M., Taconet, O., LeHegaratMasclé, S., VidalMadjar, D., Emblanch, C., Loumagne, C., et al. (1997). Backscattering behavior and simulation comparison over bare soils using SIR-C/X-SAR and ERASME 1994 data over Orgeval. *Remote Sensing of Environment*, 59, 256–266.